Spin-signal propagation in time-dependent noncollinear spin transport

Yao-Hui Zhu,* Burkard Hillebrands, and Hans Christian Schneider†
Department of Physics and Research Center OPTIMAS, University of Kaiserslautern, 67653 Kaiserslautern, Germany
(Received 6 January 2009; revised manuscript received 15 May 2009; published 10 June 2009)

Using a macroscopic analysis, we investigate the signal propagation in time-dependent noncollinear spin transport through magnetic multilayers. As in the collinear case, we find a wavelike character in addition to its diffusive character, which allows one to extract a finite spin-signal-propagation velocity. We numerically study the dynamics of a pure spin current pumped into a nonmagnetic layer by a precessing magnetization in an adjacent ferromagnetic layer for precession frequencies ranging from GHz to THz. The wave character of spin transport produces deviations from pure spin-diffusion dynamics for modulation frequencies of several 10 GHz. In this frequency range, the polarization of the pumped spin current is still approximately parallel to the injected spin at the interface at all times. Above 100 GHz, the wave character of the spin current becomes obvious because the polarization is no longer parallel to the injected spin.

DOI: 10.1103/PhysRevB.79.214412 PACS number(s): 72.25.Ba, 73.40.Jn, 75.47.−m, 85.75.−d

I. INTRODUCTION

Transporting information encoded in electronic spins through layers of ferromagnetic and normal metals is a central theme of magnetoelectronics.[1] Structures, in which all spins are essentially *collinear*, i.e., parallel or antiparallel, have been thoroughly investigated in experimental and theoretical studies. The quasistatic properties for the special case of structures with collinear spin and magnetization directions where the spin-polarized current flows perpendicularly to the plane of the layers,[2] can be analyzed in terms of a scalar space-dependent spin accumulation for up and down spins.[3,4] The functionality of collinear magnetoresistive structures can be enhanced by including tunneling elements.[5–7] Although collinear spin transport is of importance for certain variants of giant and tunneling magnetoresistance effects, a *noncollinear* alignment of spin and magnetization orientations leads to additional degrees of freedom for the manipulation of spin angular momentum and has attracted much attention in recent years.[1,8] For instance, one can exploit the angular dependence of the giant magnetoresistance effect,[9] or can change the alignment of spins by spin currents, leading to the phenomenon of spin transfer torque[10–13] and potential novel applications.[14] A different method to exploit the freedom of noncollinear spin orientations in magnetic multilayers is the use of magnetization precession in a ferromagnetic layer, which "pumps" a spin current into an adjacent nonmagnetic metal.[15] A precessing magnetization, which is necessary for spin pumping, creates the need to deal with a time-dependent orientation of the spins in the whole multilayer so that it becomes essential to study dynamical noncollinear spin transport problems.

We are concerned with a theoretical analysis of the propagation of signals encoded in a spin current, which flows through a multilayered structure with noncollinear magnetization and spin directions. Most investigations of time-dependent noncollinear spin transport are based on the Bloch-Torrey diffusion equations for the nonequilibrium magnetization or spin accumulation.[16] These equations essentially describe spin transport as a diffusion process and therefore show the same problem as the spin-diffusion equation for collinear spins:[17–20] no finite propagation velocity for a spin signal can be defined because the diffusion equation leads to a finite spin-current density everywhere as soon as there is a source. Recently, we showed that this difficulty can be resolved for collinear spin transport by using a "telegraph," or spin wave-diffusion equation, which generalizes the diffusion equation, and leads to noticeable differences from the diffusion equation results for frequencies exceeding several 100 GHz for metals such as copper.[21] Importantly, the wave-diffusion duality enables one to define a finite propagation velocity for the spin signal. In this paper, we use a similar treatment for noncollinear spin transport to show how a finite signal-propagation velocity arises in this case. We predict that noncollinear spin transport at high frequencies shows a dynamics that is more complicated than what is expected from an analysis using the spin-diffusion equation. We numerically analyze the propagation of a spin current pumped into a nonmagnetic metal by a precessing magnetization in an adjacent ferromagnetic layer.

This paper is organized as follows. In Sec. II, we present the macroscopic dynamical equations governing noncollinear spin transport. In Sec. III, the dynamical equations are combined into a wave-diffusion equation, which is studied analytically to discuss qualitative aspects of dynamical noncollinear spin transport. In Sec. IV, we solve numerically the dynamical equations for the spin transport, and the main conclusions are summarized in Sec. V.

II. DYNAMICAL EQUATIONS

In nonmagnetic conductors and some ferromagnetic metals,[22] the dynamics of conduction electrons under the influence of external fields can be described by a generalized semiclassical Boltzmann equation[23,24]

$$i\hbar\frac{\partial\hat{\rho}}{\partial t}+\frac{i}{2}\left\{\frac{\partial\hat{\varepsilon}}{\partial\vec{k}},\frac{\partial\hat{\rho}}{\partial\vec{r}}\right\}-\frac{i}{2}\left\{\frac{\partial\hat{\varepsilon}}{\partial\vec{r}},\frac{\partial\hat{\rho}}{\partial\vec{k}}\right\}=[\hat{\varepsilon},\hat{\rho}]+\left.i\hbar\frac{\partial\hat{\rho}}{\partial t}\right|_{\mathrm{col}},\tag{1}$$

which we take as the starting point for our analysis of time-dependent noncollinear electron-spin transport in these sys-

 ©2009 The American Physical Society

tems. In Eq. (1), $\hat{\rho}(\vec{r},\vec{k},t)$ is the single-particle density matrix in spin space,

$$\hat{\rho} = \begin{pmatrix} \rho_{\uparrow\uparrow} & \rho_{\uparrow\downarrow} \\ \rho_{\downarrow\uparrow} & \rho_{\downarrow\downarrow} \end{pmatrix}, \tag{2}$$

$\hat{\varepsilon}(\vec{r},\vec{k},t)$ is the effective single-particle energy matrix, and $\{\cdot,\cdot\}$ and $[\cdot,\cdot]$ denote, respectively, the anticommutator and commutator for matrices in spin space. For completeness, we remark that in Eq. (2), the single-particle density matrix

$$\rho_{ss'}(\vec{r},\vec{k},t) = \frac{V}{(2\pi)^3}\int d^3q e^{i\vec{q}\cdot\vec{r}}\langle c^{\dagger}_{\vec{k}-\vec{q}/2,s'} c_{\vec{k}+\vec{q}/2,s}\rangle, \tag{3}$$

is defined by a statistical average over creation and annihilation operators $c^{\dagger}$ and c, with normalization volume V. The diagonal matrix elements $\rho_{\uparrow\uparrow}$ and $\rho_{\downarrow\downarrow}$ are the electron distribution functions of the spin up and spin down, respectively, whereas the off-diagonal elements $\rho_{\uparrow\downarrow}=\rho^{*}_{\downarrow\uparrow}$ represent the spin coherence.[25] Because the unit matrix $\hat{I}$ and the Pauli matrices $\hat{\sigma}_x$, $\hat{\sigma}_y$, and $\hat{\sigma}_z$ form a basis for 2×2 matrices, the spin-density matrix $\hat{\rho}$ can be represented by $\hat{\rho}=(1/2)[(\rho_{\uparrow\uparrow}+\rho_{\downarrow\downarrow})\hat{I} + \vec{u}\cdot\hat{\boldsymbol{\sigma}}]$, where $\vec{u}=\mathrm{Tr}(\hat{\boldsymbol{\sigma}}\hat{\rho})=(2\ \mathrm{Re}\ \rho_{\uparrow\downarrow}, -2\ \mathrm{Im}\ \rho_{\uparrow\downarrow}, \rho_{\uparrow\uparrow}-\rho_{\downarrow\downarrow})$ is the Bloch vector and $\hat{\boldsymbol{\sigma}}$ the vector of Pauli matrices.

Before proceeding from Eq. (1) for the spin-density matrix to equations for macroscopic quantities, such as spin-current density and spin accumulation, we list a few assumptions made about quantities occurring in Eq. (1). First, we consider only layered structures whose extensions perpendicular to the growth direction (x axis) are infinite, and we also assume that the electric field $\vec{E}=E\vec{x}/|\vec{x}|$ is oriented along the growth direction $\vec{x}$. Second, the effect of magnetic fields on the orbital motion of electrons is neglected. These magnetic fields include the static external magnetic field $\vec{B}_s$ and the magnetic field generated by induction due to the time-dependent electric field $\vec{E}(x,t)$.[26] We therefore assume that the electric field $E(x,t)=-\partial\phi(x,t)/\partial x$ can be derived from a time-dependent electric potential $\phi(x,t)$. Third, an isotropic effective-mass model for the spin-degenerate conduction electrons is used, i.e., $\varepsilon_k=\hbar^2k^2/(2m^*)=m^*v^2/2$, where $\vec{k}$ and $\vec{v}$ denote the electron wave vector and velocity, respectively. Thus we have to deal with a spin-density matrix $\hat{\rho}$ that depends only on x and has cylindrical symmetry around the x axis in k space.

Finally, we make a relaxation-time approximation for the collision term[27]

$$\left.\frac{\partial\hat{\rho}}{\partial t}\right|_{\mathrm{col}} = -\frac{\hat{\rho}-\langle\hat{\rho}\rangle_a}{\tau} - \frac{\langle\hat{\rho}\rangle_a - (\hat{I}/2)\mathrm{Tr}\langle\hat{\rho}\rangle_a}{T_1}, \tag{4}$$

where τ and T_1 are the momentum and spin-relaxation times, respectively. $\langle\hat{\rho}\rangle_a \equiv (4\pi)^{-1}\int d\Omega_{\vec{k}}\hat{\rho}$ is the angular average in the momentum space. By using Eq. (4) for the collision term, we have assumed that the longitudinal spin-relaxation time T_1 is equal to the transverse one T_2. The validity of this approximation is discussed in detail by Ref. 16. Note that T_1 in Eq. (4) is one half of τ_{sf} used in Eq. (2) of Ref. 27. Moreover, Eq. (4) has used the isotropic approximation, which assumes a spherical Fermi surface for the materials. Thus, the spin-relaxation time T_1 should be understood as an average over all of the Fermi surface including the spin hot spots, which have higher spin-relaxation rates than the majority parts of the nonspherical Fermi surfaces of the materials, such as polyvalent metals.[28,29]

With above simplifications, the effective single-particle energy $\hat{\varepsilon}(\vec{r},\vec{k},t)$ is simplified to $\hat{\varepsilon}(x,|\vec{v}|,t)=\varepsilon_0\hat{I}+\hat{\varepsilon}_s$, where $\varepsilon_0=\hbar^2k^2/(2m^*)-e\phi(x,t)$ and $\hat{\varepsilon}_s=-\boldsymbol{\mu}\cdot\vec{B}_s=\mu_B\hat{\boldsymbol{\sigma}}\cdot\vec{B}_s$. Therefore, Eq. (1) simplifies to

$$\frac{\partial\hat{\rho}}{\partial t} + v_x\frac{\partial\hat{\rho}}{\partial x} - \frac{eE}{m^*}\frac{\partial\hat{\rho}}{\partial v_x} + \frac{1}{2}\gamma(\vec{u}\times\vec{B}_s)\cdot\hat{\boldsymbol{\sigma}} = -\frac{\hat{\rho}-\langle\hat{\rho}\rangle_a}{\tau} - \frac{\langle\hat{\rho}\rangle_a - (\hat{I}/2)\mathrm{Tr}\langle\hat{\rho}\rangle_a}{T_1}, \tag{5}$$

where $\gamma=g\mu_B/\hbar$ is the absolute value of the electron ($g\approx 2$) gyromagnetic ratio. This semiclassical Boltzmann equation will be used to study the spin dynamics for pumping frequencies up to 10 THz. As stressed in Ref. 23, the applicability of the Boltzmann equation is not restricted to frequencies small compared with the scattering rates, $1/\tau$ and $1/T_1$, in the collision terms of Eq. (5). In the limit $\omega\tau\ll 1$, the electrons are scattered many times during a period, whereas in the opposite limit $\omega\tau\gg 1$, the electrons may complete several cycles between two successive collisions.

To derive macroscopic spin transport equations comparable with the Bloch-Torrey diffusion equation, we need to sum over the electron wave vector $\vec{k}$ or, equivalently, the velocity $\vec{v}$ in Eq. (5). We first derive an equation for the spin density[27,30] by multiplying both sides of Eq. (5) by $\hat{\boldsymbol{\sigma}}/V$, taking the trace, and summing over $\vec{v}$,

$$\frac{\partial\vec{n}_s(x,t)}{\partial t} = -\gamma\vec{n}_s(x,t)\times\vec{B}_s - \frac{\vec{n}_s(x,t)}{T_1} - \frac{\partial\vec{J}_s(x,t)}{\partial x}, \tag{6}$$

where $\vec{n}_s(x,t)=V^{-1}\Sigma_{\vec{v}}\mathrm{Tr}(\hat{\boldsymbol{\sigma}}\hat{\rho})=V^{-1}\Sigma_{\vec{v}}\vec{u}$ and $\vec{J}_s(x,t)=V^{-1}\Sigma_{\vec{v}}v_x\,\mathrm{Tr}(\hat{\boldsymbol{\sigma}}\hat{\rho})=V^{-1}\Sigma_{\vec{v}}v_x\vec{u}$ are the spin density and spin-current density, respectively. For the spin-current density, we multiply both sides of Eq. (5) by $v_x\hat{\boldsymbol{\sigma}}/V$, take the trace, and sum over $\vec{v}$. Using the expansion [Eq. (A2)] for the velocity dependence of the spin-density matrix and the procedure in Appendix A, we obtain

$$\vec{J}_s(x,t) = -D\frac{\partial\vec{n}_s(x,t)}{\partial x} - \mu E(x,t)\vec{n}_s(x,t) - \tau\gamma\vec{J}_s(x,t)\times\vec{B}_s - \tau\frac{\partial\vec{J}_s(x,t)}{\partial t}, \tag{7}$$

where

$$D = \frac{v_F^2}{3}\tau \tag{8}$$

is the diffusion constant and $\mu=e\tau/m^*$ is the electron mobility. Note that $\vec{n}_s(x,t)$ and $\vec{J}_s(x,t)$ defined above are the particle (electron) number densities, which can be converted to the charge, spin, and magnetic-moment densities by multiplication with $-e$, $\hbar/2$, and $-\mu_B$, respectively. The spin density

$\vec{n}_s(x,t)$ can also be converted to the chemical-potential difference $\boldsymbol{\mu}_s(x,t)$, i.e., the spin accumulation, by the relation $\vec{n}_s(x,t)=\mathcal{N}\boldsymbol{\mu}_s(x,t)$, where $\mathcal{N}=4\pi m^{*2}v_F/h^3$ is the density of states at the Fermi level of the electron gas for one spin orientation.[31]

Equation (7) resembles the dynamical equation for the spin-current density derived by Qi and Zhang[27] using a "mean-field" approximation. Our derivation shows that their quantity $\overline{v_x^2}$ is equal to $c_s^2=v_F^2/3$. As will be discussed in Sec. III, c_s is the wavefront velocity for a spin disturbance, which plays an important role in spin-signal-propagation dynamics.[21]

III. WAVE-DIFFUSION EQUATION

To see the physical significance of Eqs. (6) and (7) for the time-dependent noncollinear spin transport and compare them with the Bloch-Torrey equation, we combine them by eliminating $\vec{J}_s(x,t)$ into a form reminiscent of a telegraph equation[21]

$$\begin{aligned}&\frac{\partial^2\vec{n}_s(x,t)}{\partial t^2}+\left(\frac{1}{\tau}+\frac{1}{T_1}\right)\frac{\partial\vec{n}_s(x,t)}{\partial t}+\frac{\vec{n}_s(x,t)}{\tau T_1}\\&+\gamma\left[2\frac{\partial}{\partial t}+\left(\frac{1}{\tau}+\frac{1}{T_1}\right)\right]\vec{n}_s(x,t)\times\vec{B}_s\\&+\gamma^2[\vec{n}_s(x,t)\times\vec{B}_s]\times\vec{B}_s\\&=c_s^2\frac{\partial^2\vec{n}_s(x,t)}{\partial x^2}+\frac{\mu E(x,t)}{\tau}\frac{\partial\vec{n}_s(x,t)}{\partial x}+\frac{\mu}{\tau}\frac{\partial E(x,t)}{\partial x}\vec{n}_s(x,t).\end{aligned}\tag{9}$$

Similarly, one can also derive an equation for $\vec{J}_s(x,t)$ by eliminating $\vec{n}_s(x,t)$ from Eqs. (6) and (7). Equation (9) can be called a "spin wave-diffusion equation" because it contains an additional second-order time derivative, which is absent in the spin-diffusion equation. The second-order time and space derivatives lead to a wave character in addition to its diffusion character and thus yield a well-defined propagation velocity $c_s=v_F/\sqrt{3}$ for the signal in time-dependent noncollinear spin transport in a similar way to the collinear case.[21]

Assuming the static magnetic field $\vec{B}_s$ to be oriented along the z axis and separating the components perpendicular (transverse) and parallel (longitudinal) to $\vec{B}_s$ in Eq. (9), we have

$$\begin{aligned}&\frac{\partial^2 n_s^{x(y)}}{\partial t^2}+\left(\frac{1}{\tau}+\frac{1}{T_1}\right)\frac{\partial n_s^{x(y)}}{\partial t}+\frac{n_s^{x(y)}}{\tau T_1}\\&+(-)\gamma B_s\left[2\frac{\partial}{\partial t}+\left(\frac{1}{\tau}+\frac{1}{T_1}\right)\right]n_s^{y(x)}-\gamma^2B_s^2n_s^{x(y)}\\&=c_s^2\frac{\partial^2 n_s^{x(y)}}{\partial x^2}+\frac{\mu E}{\tau}\frac{\partial n_s^{x(y)}}{\partial x}+\frac{\mu}{\tau}\frac{\partial E}{\partial x}n_s^{x(y)}\end{aligned}\tag{10}$$

and

$$\frac{\partial^2 n_s^z}{\partial t^2}+\left(\frac{1}{\tau}+\frac{1}{T_1}\right)\frac{\partial n_s^z}{\partial t}+\frac{n_s^z}{\tau T_1}=c_s^2\frac{\partial^2 n_s^z}{\partial x^2}+\frac{\mu E}{\tau}\frac{\partial n_s^z}{\partial x}+\frac{\mu}{\tau}\frac{\partial E}{\partial x}n_s^z.\tag{11}$$

In the following, only the equations for the transverse component [Eq. (10)] will be discussed since the equation for the longitudinal component is similar to that of the collinear case.[21] For vanishing electric field, i.e., $E=0$, we seek damped and dispersive wave solutions to Eq. (10) of the form

$$n_s^x(x,t)=n_0\exp[i(kx-\omega t)],\tag{12}$$

$$n_s^y(x,t)=n_0\exp[i(kx-\omega t+\phi)],\tag{13}$$

where ω is the angular frequency and $k=k_r+ik_i$ the complex wave vector. Substituting Eqs. (12) and (13) into Eq. (10), we obtain the dispersion relation

$$\begin{aligned}&\omega^2+i\omega(1/\tau+1/T_1)-1/(\tau T_1)-c_s^2k^2+\gamma^2B_s^2\\&-\gamma B_s[2\omega+i(1/\tau+1/T_1)]\sin\phi=0,\end{aligned}\tag{14}$$

where ϕ is restricted to $\phi=\pm(\pi/2)+2n\pi$ and n is an integer because n_s^x and n_s^y must satisfy the two coupled equations shown by Eq. (10) at the same time. According to Eqs. (12) and (13), $\phi=+(-)\pi/2$ corresponds to the rotation direction of the transverse component of $\vec{n}_s(x,t)$ with x at time t. For definiteness, we study the case with $\phi=\pi/2$ in the following. Substituting $k=k_r+ik_i$ into Eq. (14) and separating the real and imaginary parts, we have

$$k_{r(i)}^2=\frac{1}{2c_s^2}[\sqrt{b^2+\omega_{\mathrm{eff}}^2\alpha^2}+(-)b],\tag{15}$$

where $\omega_{\mathrm{eff}}=\omega-\gamma B_s$ and $b=\omega_{\mathrm{eff}}^2-\xi$. Here, the constants $\alpha=1/\tau+1/T_1$ and $\xi=1/(\tau T_1)$ have been introduced. The wavelength and damping length can be defined as $\lambda=2\pi/k_r$ and $l_d=1/k_i$, respectively. The equation of the critical angular frequency ω_{crit}, above which the wave character is significant, can be derived by setting $\lambda=l_d$,

$$\omega_{\mathrm{eff}}^{\mathrm{crit}}\tau=\frac{1}{2}[\delta(1+\eta)+\sqrt{\delta^2(1+\eta)^2+4\eta}]\approx\delta+\left(\delta+\frac{1}{\delta}\right)\eta,\tag{16}$$

where $\delta=\pi-1/(4\pi)\approx3.06$ and $\eta=\tau/T_1$. Then, we have $\omega_{\mathrm{crit}}\tau=3.06+3.4\eta+\tau\gamma B_s$ approximately.

IV. DYNAMICS OF PUMPED SPIN CURRENT

In this section, we study the evolution of the spin current injected into a nonmagnetic layer by the spin-pumping mechanism.[15] In a junction composed of a ferromagnetic ($x<0$) and a nonmagnetic ($x>0$) layer, the magnetization precession of the ferromagnet around an external magnetic field $\vec{B}_{\mathrm{pump}}$ acts as a "spin pump" which transfers spin angular momentum from the ferromagnet to the adjacent nonmagnetic layer. The spin-current density pumped into the nonmagnetic layer is[15,31,32]

$$\vec{J}_s^{\text{pump}} = \frac{1}{2\pi}\frac{g^{\uparrow\downarrow}}{S}\vec{m}\times\frac{d\vec{m}}{dt}, \tag{17}$$

where $g^{\uparrow\downarrow}$ is the spin-mixing conductance and S is the area of the interface. Here, $\vec{m}$ is the unit vector for the magnetization of the ferromagnet. Note that the pumped spin current has been converted to a particle number current density $\vec{J}_s^{\text{pump}}$. Since we are interested in the spin current pumped into a nonmagnetic layer and not in the dynamics of the ferromagnet, we neglect the back-flow spin current $\vec{I}_s^{\text{back}}$, which flows from the nonmagnetic layer to the ferromagnet due to the spin accumulation in the nonmagnetic layer.[31] Although the back-flow spin current can limit the achievable spin current into the nonmagnetic conductor, we do not approach this limit here. With this simplification, we have $\vec{J}_s^{\text{pump}}=\vec{J}_s(x=0,t)$, where $\vec{J}_s(x=0,t)$ is the spin-current density at the left boundary of the nonmagnetic layer. Separating the components perpendicular and parallel to the magnetic field $\vec{B}_{\text{pump}}$, we can write $\vec{J}_s(x=0,t)$ as

$$j_s^x(x=0,t) = g^{\uparrow\downarrow}(4\pi S)^{-1}\omega\sin(2\theta)\cos(\omega t), \tag{18}$$

$$j_s^y(x=0,t) = g^{\uparrow\downarrow}(4\pi S)^{-1}\omega\sin(2\theta)\sin(\omega t), \tag{19}$$

$$j_s^z(x=0,t) = g^{\uparrow\downarrow}(2\pi S)^{-1}\omega\sin^2\theta, \tag{20}$$

where ω is the angular frequency of both the magnetization precession and the spin-current density $\vec{J}_s(x=0,t)$. Here, ωt is the angle between $\vec{J}_s^{\perp}$ (j_s^x and j_s^y) and the x axis, and θ is the angle between $\vec{m}$ and $\vec{B}_{\text{pump}}$, so that θ is also the angle between $\vec{J}_s(x=0,t)$ and the xy plane. The amplitude of $\vec{J}_s^{\perp}$ is much larger than j_s^z since θ is very small under the usual radio-frequency excitation conditions.[32] Therefore, we will focus on $\vec{J}_s^{\perp}$ in the following.

The propagation of $\vec{J}_s^{\perp}(x=0,t)$ into the nonmagnetic layer is described by Eqs. (6) and (7). In a typical setup for spin pumping, there is no electric or magnetic field in the nonmagnetic layer, i.e., $E=0$ and $\vec{B}_s=0$. Now, separating the components perpendicular and parallel to the magnetic field $\vec{B}_{\text{pump}}$, we can rewrite Eqs. (6) and (7) as

$$\frac{\partial n_s^+}{\partial t}+\frac{\partial j_s^+}{\partial x}=-\frac{n_s^+}{T_1}, \tag{21}$$

$$j_s^+ = -D\frac{\partial n_s^+}{\partial x}-\tau\frac{\partial j_s^+}{\partial t}, \tag{22}$$

where $n_s^+=n_s^x+in_s^y$ and $j_s^+=j_s^x+ij_s^y$ are introduced to simplify the notations. The equations for the parallel component can be obtained after replacing n_s^+ and j_s^+ by n_s^z and j_s^z in Eqs. (21) and (22), respectively. The method of characteristics used for the numerical solution to Eqs. (21) and (22) is outlined in Appendix B.

In our numerical calculation, Cu and permalloy (Py) are chosen as the materials for the nonmagnetic and ferromagnetic layers, respectively. The Fermi velocity of Cu is $v_F=1570$ nm/ps and thus the wave-front velocity is $c_s=v_F/\sqrt{3}=906$ nm/ps. The momentum and spin-relaxation

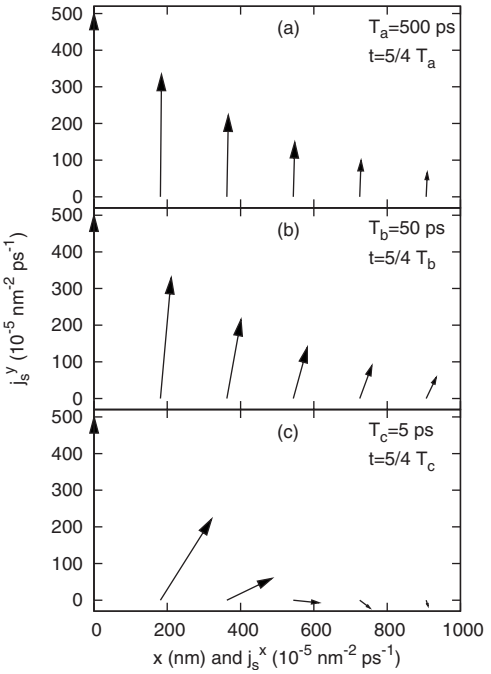

FIG. 1. Snapshots of the spin-current density $\vec{J}_s^{\perp}$ at $t=5/4\ T_a$, $5/4T_b$, and $5/4T_c$, for the frequencies, ν_a, ν_b, and ν_c, respectively (see text). $\vec{J}_s^{\perp}$ is plotted as vector starting from its x coordinate.

times are $\tau=0.07$ ps and $T_1=3.5$ ps, respectively.[21] The critical frequency can be estimated to be $\nu_{\text{crit}}=\omega_{\text{crit}}/(2\pi)=7.11$ THz from Eq. (16). We study several pumping frequencies: $\nu_a=1/T_a=2$ GHz, $\nu_b=1/T_b=20$ GHz, $\nu_c=1/T_c=200$ GHz, and $\nu_d=1/T_d=8.33$ THz. For a Py/Cu junction,[31] $g^{\uparrow\downarrow}S^{-1}$ is on the order of 10^{15} cm^{-2}. The precession cone angle θ can reach 15° for a sufficiently intense radio-frequency field.[32] Therefore, we choose the amplitude of $\vec{J}_s^{\perp}$, i.e., $g^{\uparrow\downarrow}(4\pi S)^{-1}\omega\sin(2\theta)$, to be 5×10^{-3} nm^{-2} ps^{-1} for the frequencies mentioned above.

Figure 1 shows snapshots of the spin-current density $\vec{J}_s^{\perp}$ at $t=(5/4)T_a$, $(5/4)T_b$, and $(5/4)T_c$, for the frequencies, ν_a, ν_b, and ν_c, respectively. According to Eqs. (18) and (19), we have $j_s^x(x=0,t)=0$ and $j_s^y(x=0,t)=|\vec{J}_s^{\perp}(x=0,t)|$ at $t=(5/4)T_{a(b,c)}$, and so $\vec{J}_s^{\perp}(x=0,t)$ points in the direction of the y axis, which can also be seen in Fig. 1. Figure 1(a) shows that $\vec{J}_s^{\perp}(x,t)$ points along y axis nearly everywhere except far away from the interface. The results in Fig. 1(a) are approximately consistent with those obtained from the diffusion equation in Refs. 31 and 32, where it is shown that both the spin-current density and spin accumulation point along the same direction at all positions for all frequencies for any given time t. According to diffusion theory, $\vec{J}_s^{\perp}(x,t)$ should point along y axis everywhere at $t=(5/4)T_{a,(b,c)}$. The deviation of $\vec{J}_s^{\perp}$ from the y axis at $x>0$ is an indication how much the spin-current dynamics shown here differs from the corresponding spin-diffusion result. Figure 1(a) therefore indicates that the diffusion equation provides a good description of the time-dependent spin transport in the low-frequency range.[33] The deviation of the direction of $\vec{J}_s^{\perp}$ for $x>0$ increases with frequency and becomes noticeable at $\nu_b=1/T_b=20$ GHz as shown in Fig. 1(b). Starting around this fre-

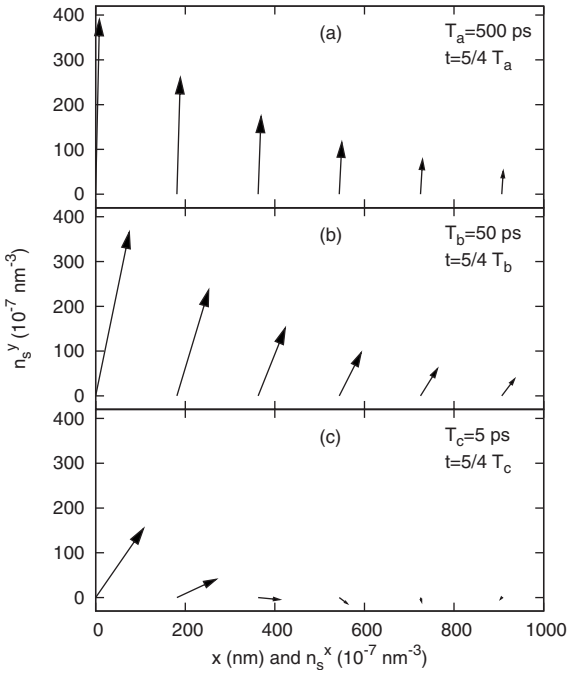

FIG. 2. Snapshots of the spin density $\vec{n}_s^{\perp}$ for the same parameters as in Fig. 1.

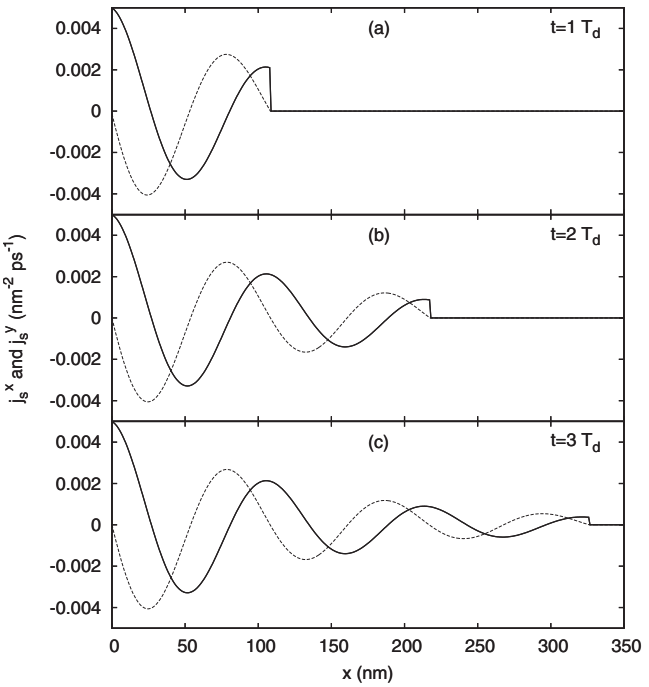

FIG. 3. Snapshots of $\vec{J}_s^{\perp}$ at $t=T_d$, $2T_d$, and $3T_d$, where $T_d=0.12$ ps. The solid (dashed) curve is for j_s^x (j_s^y).

quency, the applicability of the diffusion equation becomes questionable. For even higher frequencies, such as $\nu_c=1/T_c=200$ GHz shown in Fig. 1(c), the dynamical spin current exhibits two new important features. First, the direction of the spin-current vector shows a strong x dependence, which is a qualitative difference to the spin-diffusion result. Physically this behavior is due to finite propagation velocity c_s, which results in a phase difference of $\vec{J}_s^{\perp}$ at $x=0$ and $x=x_0>0$: $\delta\phi\approx(x_0/c_s)\omega$, where ω is the angular frequency of $\vec{J}_s^{\perp}(x=0,t)$. In spin-diffusion theory, $\delta\phi$ is zero for all values of x and ω because of its unphysical infinite spin-signal-propagation velocity. The phase shift $\delta\phi$ increases with both x_0 and frequency, as can be seen from Fig. 1. Second, Fig. 1 shows that the penetration depth of the spin current decreases with frequency. This is reminiscent of the Hanle effect for spin *diffusion* in a magnetic field, where the penetration depth also decreases with the Larmor frequency. This effect can be explained by a random-walk model for the diffusion process, in which the precessing electronic spins acquire different phases along their walk.[34] However, since the spin-current dynamics shown in Fig. 1 is a *wave-diffusion* dynamics, it is likely more appropriate to explain the decreasing penetration depth at higher frequencies by the "skin effect" inherent in the wave-diffusion equation.[21]

Figure 2 shows snapshots of the spin density $\vec{n}_s^{\perp}$ for the same parameters as in Fig. 1. The spin density $\vec{n}_s^{\perp}$ deviates from the y axis everywhere even directly at the interface and is noncollinear with $\vec{J}_s^{\perp}$ at any x point for all of the three frequencies. This feature is different from the result of the diffusion equation, where $\vec{J}_s^{\perp}$ and $\vec{n}_s^{\perp}$ are collinear.[31,32] The phase shift of $\vec{n}_s^{\perp}$ also varies with frequency. These features result from the wave characteristics of the time-dependent spin transport. To see this, let us look at Eq. (7) and (22). The wave characteristics originate from the last term of Eq. (7) and (22), which is absent in the corresponding equation for the spin-current density in the spin-diffusion theory [see, for instance, Eq. (9) in Ref. 31]. This additional term means that there is no instantaneous relation between j_s^+ and n_s^+ ($\vec{J}_s^{\perp}$ and $\vec{n}_s^{\perp}$) but the dynamics is influenced by the finite relaxation time τ. Therefore, $\vec{J}_s^{\perp}$ and $\vec{n}_s^{\perp}$ have enough time to adjust and become almost collinear at low frequency $\nu\ll\nu_{\mathrm{crit}}$, where the signal varies slowly enough. At higher frequencies, comparable with ν_{crit}, there is not enough time for $\vec{J}_s^{\perp}$ and $\vec{n}_s^{\perp}$ to become essentially collinear. Moreover, comparing the results of the three frequencies in Fig. 2, one can also see that the amplitude of $\vec{n}_s^{\perp}$ decreases with frequency. The reason is that the signal varies faster at higher frequency so that the spin density has less time to reach its maximum amplitude. As pointed out above for the spin-current density, the penetration depth of $\vec{n}_s^{\perp}$ decreases with frequency due to the "skin" effect.

According to Eq. (16), the diffusion character is dominant at the frequencies considered so far because they are still smaller than the critical frequency ν_{crit}. This conclusion is supported by the numerical results presented in Figs. 1 and 2, although Figs. 1(c) and 2(c) have already shown weak wavelike character. The deviation from the diffusion equation depends largely on the frequency of the spin signal and momentum relaxation time, which varies with material, temperature, doping, and excitation condition. In the following, we show the numerical results for a frequency $\nu_d=8.33$ THz, where the wave character is significant according to Eq. (16).

Figure 3 shows snapshots of the spin-current density $\vec{J}_s^{\perp}$ at $t=1T_d$, $2T_d$, and $3T_d$, respectively. The wave form and wave front are clearly visible in Fig. 3. The propagation velocity of

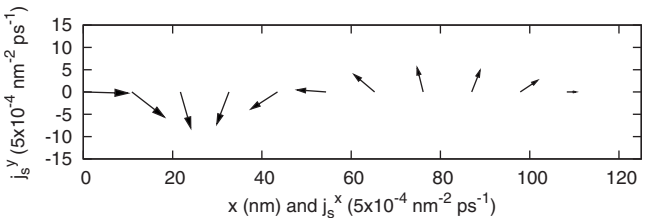

FIG. 4. Snapshot of $\vec{j}_s^{\perp}$ (plotted as vector) at $t=T_d$.

the spin signal can be estimated by tracking the motion of the wave front. The result is approximately equal to the analytical result $c_s=906$ nm/ps. The phase velocity can also be estimated by measuring the wavelength λ and using $v_p=\lambda/T_d$. The result is roughly equal to the wave-front velocity c_s, which also indicates the significance of the wave character, albeit on the length scale of the damping length (dynamical spin-diffusion length). To demonstrate the wave character more directly, we plot the results of Fig. 3(a) again in Fig. 4, where $\vec{j}_s^{\perp}$ is shown in a vector plot. Note that ν_d is beyond the frequency range in which Eq. (17) is valid because Eq. (17) is only applicable in the adiabatic limit, $\nu \ll 1/\tau$.[15] Unfortunately, there is no corresponding theoretical result for the nonadiabatic spin pumping in the literature. However, it is a reasonable guess that the pumped spin-current density in the nonadiabatic regime preserves the basic feature of Eq. (17): $\vec{j}_s^{\text{pump}}$ rotates with a certain fixed frequency. Therefore, the spin-current density predicted by our results should be at least qualitatively accurate in this frequency range.

V. SUMMARY AND OUTLOOK

We showed that time-dependent noncollinear spin transport exhibits a wave character for modulation of the spin current on timescales shorter than an inverse critical frequency. A finite propagation velocity, $c_s=v_F/\sqrt{3}$, for the spin signal can be defined due to this wave character. The spin-diffusion equation is recovered only for modulation with frequencies much lower than the critical frequency ν_{crit}, and amounts to an adiabatic approximation of time-dependent spin transport, where the external perturbation is assumed to be much slower than the internal dynamics of the electronic system. We numerically studied the dynamics of a spin current pumped by a precessing magnetization in a Py layer into an adjacent Cu layer. We found a pronounced space dependence of the direction of the spin current at high frequencies ($\nu \geq 100$ GHz), accompanied by a reduced penetration depth. Both of these features are due to the wave character of the spin-current dynamics.

In closing, we would like to comment on the relevance of our results for experimental investigations. The frequencies, for which we find the most pronounced effects, are in a range that is beyond present-day electronics, and can only be reached in metallic nanostructures by optical means.[35] A different possible experimental verification of our theory is the measurement of the spin-signal-propagation velocity, which is $c_s=v_F/\sqrt{3}$. Such a measurement is independent of the frequency or time scale of the signal. Further, we are currently analyzing in which systems, e.g., nanostructures and doped semiconductors, and for which experimental setups our theory predicts corrections to the spin-diffusion theory or effects outside spin-diffusion theory, such as standing waves.

ACKNOWLEDGMENTS

We acknowledge financial support from the state of Rheinland-Pfalz through the MATCOR program and a CPU-time grant from the John von Neumann Institut for Computing (NIC) at the Forschungszentrum Jülich. We thank G.E.W. Bauer for helpful discussions.

APPENDIX A: DERIVATION

Equations (6) and (7) of Ref. 27 are derived using the "mean field" approximation

$$\sum_{\vec{v}} v_x^2(\partial\hat{\rho}/\partial x) \approx \overline{v_x^2}\sum_{\vec{v}} (\partial\hat{\rho}/\partial x). \tag{A1}$$

Here we show that $\overline{v_x^2}=c_s^2$ by evaluating the sums occurring in Eq. (A1). We start with the left-hand side (LHS), which we denote by $I_1=\Sigma_{\vec{v}} v_x^2(\partial\hat{\rho}/\partial x)$. Due to the cylindrical symmetry of the system around the x axis in velocity space, $\hat{\rho}$ can be expanded in Legendre polynomials of $u=\cos\theta$, where θ is the angle between $\vec{v}$ and the x axis, as

$$\hat{\rho} = \sum_{n=0}^{\infty} \hat{\rho}_n(v,x)P_n(u). \tag{A2}$$

Transforming the summation into an integral, we have

$$I_1 = \frac{2\pi V m^{*3}}{h^3}\int_{-1}^{1} duu^2 \int_0^{\infty} dvv^4 \sum_{n=0}^{\infty} \frac{\partial}{\partial x}\hat{\rho}_n(v,x)P_n(u). \tag{A3}$$

Using $u^2=[2P_2(u)+P_0(u)]/3$, we write the integral as

$$I_1 = \frac{2\pi V m^{*3}}{h^3}\int_0^{\infty} dvv^4 \sum_{n=0}^{\infty} \frac{\partial}{\partial x}\hat{\rho}_n(v,x) \times \int_{-1}^{1} du\frac{1}{3}[2P_2(u)+P_0(u)]P_n(u). \tag{A4}$$

Making use of the orthogonality relation of Legendre polynomials, we have

$$I_1 = \frac{2\pi V m^{*3}}{h^3}\int_0^{\infty} dvv^4 \frac{\partial}{\partial x}\left[\frac{4}{15}\hat{\rho}_2(v,x)+\frac{2}{3}\hat{\rho}_0(v,x)\right]. \tag{A5}$$

If the system is weakly anisotropic, we can neglect the second-order term $\hat{\rho}_2(v,x)$,

$$I_1 \approx \frac{4\pi V m^{*3}}{3h^3}\int_0^{\infty} dvv^4 \frac{\partial}{\partial x}\hat{\rho}_0(v,x). \tag{A6}$$

This approximation is consistent with Ref. 4, where the second-order term of the Legendre polynomials is neglected

and it is shown that this is valid if $\sqrt{\tau/(2T_1)} \ll 1$.

Because $\partial\hat{\rho}_0(v,x)/\partial x$ is zero unless v falls in a small region $[v_F-\Delta v, v_F+\Delta v]$ around the Fermi velocity v_F of a system with a degenerate electron gas, we have approximately

$$I_1 = \frac{4\pi V m^{*3}}{h^3}\frac{v_F^2}{3}\int_{v_F-\Delta v}^{v_F+\Delta v} dv v^2 \frac{\partial}{\partial x}\hat{\rho}_0(v,x)$$
$$= \frac{v_F^2}{3}\frac{4\pi V m^{*3}}{h^3}\int_0^{\infty} dv v^2 \frac{\partial}{\partial x}\hat{\rho}_0(v,x). \quad \text{(A7)}$$

We now need to evaluate the right-hand side (RHS) of Eq. (A1), which we denote by

$$I_2 = \overline{v_x^2}\frac{V m^{*3}}{h^3} 2\pi \int_{-1}^{1} du \int_0^{\infty} dv v^2 \frac{\partial}{\partial x}\hat{\rho}(\vec{v},x)$$
$$= \overline{v_x^2}\frac{4\pi V m^{*3}}{h^3}\int_0^{\infty} dv v^2 \frac{\partial}{\partial x}\hat{\rho}_0(v,x), \quad \text{(A8)}$$

where in the last line, we used that the integral over u projects the contribution of P_0 out of $\hat{\rho}(\vec{v},x)$. Because $I_1 = I_2$, we conclude that $\overline{v_x^2} = v_F^2/3 \equiv c_s^2$.

APPENDIX B: NUMERICAL SOLUTION

The basics of our numerical method have been outlined in Appendix A4 of Ref. 21. For present calculation, it has to be augmented by a discretized version of the boundary condition on at ferromagnet/nonmagnet interface,

$$(\Delta t/T_1 + 2)n_{s,i}^{+,l+1} = -(\Delta t/T_1 - 2)n_{s,i+1}^{+,l} + c_s^{-1}(\Delta t/\tau - 2)j_{s,i+1}^{+,l}$$
$$+ c_s^{-1}(\Delta t/\tau + 2)j_{s,i}^{+,l+1}, \quad \text{(B1)}$$

where the subscripts i and superscripts l stand for the discrete space-time points and Δt is the numerical time step.

*yaohuizhu@gmail.com
†http://www.physik.uni-kl.de/schneider

[1] A. Brataas, G. E. W. Bauer, and P. J. Kelly, Phys. Rep. **427**, 157 (2006).
[2] W. P. Pratt, Jr., S.-F. Lee, J. M. Slaughter, R. Loloee, P. A. Schroeder, and J. Bass, Phys. Rev. Lett. **66**, 3060 (1991).
[3] P. C. van Son, H. van Kempen, and P. Wyder, Phys. Rev. Lett. **58**, 2271 (1987).
[4] T. Valet and A. Fert, Phys. Rev. B **48**, 7099 (1993).
[5] G. Schmidt, D. Ferrand, L. W. Molenkamp, A. T. Filip, and B. J. van Wees, Phys. Rev. B **62**, R4790 (2000).
[6] E. I. Rashba, Phys. Rev. B **62**, R16267 (2000).
[7] A. Fert and H. Jaffrès, Phys. Rev. B **64**, 184420 (2001).
[8] Y. Tserkovnyak, A. Brataas, G. E. W. Bauer, and B. I. Halperin, Rev. Mod. Phys. **77**, 1375 (2005).
[9] J. Barnaś, O. Baksalary, and A. Fert, Phys. Rev. B **56**, 6079 (1997).
[10] J. C. Slonczewski, J. Magn. Magn. Mater. **159**, L1 (1996).
[11] L. Berger, Phys. Rev. B **54**, 9353 (1996).
[12] M. Tsoi, A. G. M. Jansen, J. Bass, W.-C. Chiang, M. Seck, V. Tsoi, and P. Wyder, Phys. Rev. Lett. **80**, 4281 (1998).
[13] E. B. Myers, D. C. Ralph, J. A. Katine, R. N. Louie, and R. A. Buhrman, Science **285**, 867 (1999).
[14] J. A. Katine and E. E. Fullerton, J. Magn. Magn. Mater. **320**, 1217 (2008).
[15] Y. Tserkovnyak, A. Brataas, and G. E. W. Bauer, Phys. Rev. Lett. **88**, 117601 (2002).
[16] I. Žutić, J. Fabian, and S. Das Sarma, Rev. Mod. Phys. **76**, 323 (2004), in particular, Sec. IIIA1.
[17] S. Zhang and P. M. Levy, Phys. Rev. B **65**, 052409 (2002).
[18] E. I. Rashba, Appl. Phys. Lett. **80**, 2329 (2002).
[19] J. Zhang and P. M. Levy, Phys. Rev. B **71**, 184417 (2005).
[20] Ł. Cywiński, H. Dery, and L. J. Sham, Appl. Phys. Lett. **89**, 042105 (2006).
[21] Y.-H. Zhu, B. Hillebrands, and H. C. Schneider, Phys. Rev. B **78**, 054429 (2008).
[22] J. Zhang, P. M. Levy, S. Zhang, and V. Antropov, Phys. Rev. Lett. **93**, 256602 (2004).
[23] H. Smith and H. H. Jensen, *Transport Phenomena* (Clarendon, Oxford, 1989).
[24] J. Rammer and H. Smith, Rev. Mod. Phys. **58**, 323 (1986).
[25] L. J. Sham, J. Magn. Magn. Mater. **200**, 219 (1999).
[26] N. W. Ashcroft and N. D. Mermin, *Solid State Physics* (Brooks/Cole, Belmont, CA, 1976).
[27] Y. Qi and S. Zhang, Phys. Rev. B **67**, 052407 (2003).
[28] J. Fabian and S. Das Sarma, Phys. Rev. Lett. **81**, 5624 (1998).
[29] M. Johnson, Semicond. Sci. Technol. **17**, 298 (2002).
[30] A. D. Margulis and V. A. Margulis, Physica B **193**, 179 (1994).
[31] Y. Tserkovnyak, A. Brataas, and G. E. W. Bauer, Phys. Rev. B **66**, 224403 (2002).
[32] A. Brataas, Y. Tserkovnyak, G. E. W. Bauer, and B. I. Halperin, Phys. Rev. B **66**, 060404(R) (2002).
[33] T. Gerrits, M. L. Schneider, and T. J. Silva, J. Appl. Phys. **99**, 023901 (2006).
[34] J. Fabian, A. Matos-Abiague, C. Ertler, P. Stano, and I. Žutić, Acta Phys. Slovaca **57**, 565 (2007).
[35] M. A. Seo *et al.*, Nat. Photonics **3**, 152 (2009).